Refractive index sensor based on tapered photonic crystal fiber to determine the performance of different carbonated liquids

Sally K. Abbas[1] · Soudad S. Ahmed[1]

Abstract   In this work, a single mode fiber (SMF) is spliced with a photonic crystal fiber (ESM-12) from both sides and tapered down to (92.1 μm) to create a surface plasmon resonance (SPR) based on Mach–Zehnder interferometer for the purpose of calculating the refractive indices of Carbonated liquids with different expiration dates. The (SMF-PCF-SMF) sensor is coated with gold film (Au) of 40 nm thickness on the stripped part of the spliced PCF to optimize the sensing performance of the fiber. The sensor has a sensitivity of (7.17) (μm/RIU), figure of merit is (19.14), signal-to-noise ratio of (0.536), and resolution of (1.3×10^{-4}) (RIU).

Keywords   Tapering · Photonic crystal fiber · Mach–Zehnder interferometer · Carbonated liquids

Introduction

Optical fiber technology is widely used in various fields today, including telecommunications, medicine, and scientific research, and over the past few decades, significant technological advancements have enabled new applications to be developed [1]. The ability to efficiently restrict and guide high intensity optical modes at certain frequencies inside an air-guided. optical fiber has made photonic crystal fibers the subject of considerable research and commercial applications. As a result of this principle, it is possible to create "endless single mode optical fibers," low loss guiding optical fibers, and optical fibers with large core areas, among other versatile designs [2]. PCFs are comparable to regular optical fibers in that they comprise of a core encircled by cladding, permitting light to pass right through the core. An important distinction between PCFs and ordinary optical fibers is that PCFs possess air-silica cross sections, whereas standard optical fibers possess glass cross sections [3]. Based on their light-guiding mechanisms, PCFs are categorized as Solid Core Photonic Crystal Fibers with Modified Total Internal Reflection, and Hollow Core Photonic. Crystal Fibers with Photonic Band. Gap [4].

In SPR, surface plasmon polaritons (SPPs) oscillate at any metal–dielectric interface when they receive maximum energy from an external source. The electrical shock is caused by polarized light at the metallic-dielectric junction in the plasma optical excitation effect [5]. The ability of surface plasmons to sense variations in the refractive index of encircling medium has made SPR a promising sensor technology in chemistry, biomedicine, and environmental monitoring [6–9].

SPR sensing with PCFs with a range of air holes along the propagation path is appealing due to their structural elasticity [10–12]. SPR sensors based on PCFs (PCF-SPRs) are based on phase matching among the core-guided and surface plasmon polaritons (SPPs) modes.

A PCF with index-guiding properties, also called a holey fiber or a microstructure fiber, exhibits an attractive property of controlling chromatic dispersion by varying the diameter and spacing between the holes [13, 14]. Higher-order mode cutoffs at short wavelengths and macro bending losses at long frequencies typically restrict the bandwidth of typical Single-mode fibers' (SMF). To fully utilize PCFs, conventional single-mode fibers' light must be effectively coupled to them. Despite this, conventional

✉ Sally K. Abbas
Sallyaljanabi@gmail.com

Soudad S. Ahmed
soudadbassam@gmail.com

1 Department of Physics, College of Science, University of Baghdad , Baghdad, Iraq

fibers' microhole structures make it difficult to splice various PCFs together. Microhole collapse, a brand-new problem that is crucial to our comprehension of splice loss. To discover new splice methods between these diverse types of fibers, an organized examination needs to be shown, which has not been done so far [15].

Due to their compact size, high sensitivity, electrical passiveness, immunity to electromagnetic interference, wide bandwidth, and convenience for tip-based sensing, optical fiber sensors are widely used in science, environmental monitoring, and communication technology. In most cases, these optical sensors measure the variations in optical properties resulting from changes in the refractive index (RI) of a gas or liquid [16]. It is very important to measure the RI of fluids in order to illustrate the optical properties of fluids, leading to the development of RI sensors for applications in many fields, including the measurement of water salinity, and biotechnology processes provide valuable information on how drugs interact with DNA and how cells grow [17]. Among the difficulties that sensors may face are their cost, the amount of the sample to be sensitive, the sensor's size, and its performance properties, such as its signal-to-noise ratio, sensitivity, and resolution. A sensor's sensitivity can be enhanced by using plasmonic materials, such as gold and silver. When it is exposed to air, silver loses its chemical stability. On the other hand, gold is a preferred plasmonic material because to its chemical stability and strong resonance peak [18]. Using PCF-SPR, an evanescent field can be used as a sensing mechanism. Evanescent fields are created when light of a specific wavelength passes through the cladding and hits the fiber core of the PCF. The surface plasmon wave is created when evanescent fields interact with free electrons in a plasmonic metal layer such as silver, gold, copper, and aluminum [19]. To monitor variations in the refractive index (RI) of carbonated liquids, a photonic crystal fiber tapered sensor based on SPR with a gold layer coating in the center was created.

Tapering diameter of photonic crystal fiber

Tapering of optical fibers by etching is a technique used to reduce the diameter of a section of an optical fiber gradually. This process involves controlled chemical or plasma etching to remove material from the fiber's cladding or core, resulting in a tapered region with a smaller cross-sectional area. After tapering, the tapered fiber was placed on a glass slide and subjected to an optical microscope to measure the SMF-PCF-SMF diameter. The tapering process was done by using Hydrofluoric acid, and Fig. 1 shows the effect of this acid on the fiber which leads to a decrease in the fiber diameter from 125 to 92.1 μm.
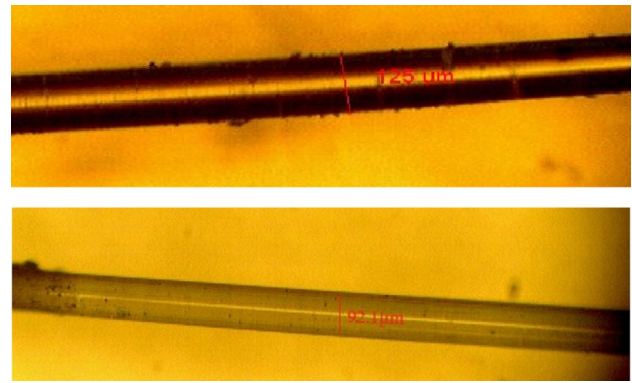

Fig. 1 Shows the images of Photonic crystal fiber before and after it is tapered to 91 μm in diameter

Fig. 2 Splicing of PCF and SMF by means of fusion splicer

Design and construction of the Mach–Zehnder interferometer sensor

This arrangement requires the splicing of photonic crystal fiber and another type of fiber which will be single mode fiber. Splicing a Photonic Crystal Fiber (PCF) with a single-mode fiber (SMF) requires careful alignment and fusion techniques to ensure efficient light coupling between the two fibers. The splicing process was done via a fusion splicer (Shinho s16) with the SMF spliced on both sides of PCF and the sensing region of PCF was 4cm long. In this work, a (ESM-12) PCF was selected due to its high sensitivity to environmental changes, including temperature, strain, pressure and refractive index. The PCF's large evanescent field and long interaction length with the external environment enhance the sensitivity of the sensing mechanism with single mode fiber alongside the PCF which is easy to install and maintain as seen in Fig. 2.

Performance parameter

There are a number of parameters that can be used to estimate the performance of PCF-SPR sensors, including

sensitivity, resolution, signal-to-noise ratio, and figure of merit:

The sensitivity of a sensor refers to how much its output changes in response to a given change in the input parameter being measured. In the context of an optical sensor based on a resonance wavelength, the sensitivity is a measure of how much the resonance wavelength shifts for a small change in the parameter being sensed (e.g., temperature, strain, refractive index, etc.).

The sensitivity formula for the resonance wavelength of an optical sensor can be expressed as follows [16]:

$$S_\lambda \left[\frac{\text{nm}}{\text{RIU}}\right] = \frac{\Delta \lambda_{\text{peak}}}{\Delta n_a} \quad (1)$$

where $\Delta \lambda_{\text{peak}}$ and Δn_a are the difference in the wavelength resonance peak and difference in the RI of the two neighboring analytes, correspondingly.

The equation below may be used to compute the resolution (R) of a sensor, which shows how much minor fluctuation in analyte RI can be seen. [17]:

$$R[\text{RIU}] = \Delta n_a \times \frac{\Delta \lambda_{\text{min}}}{\Delta \lambda_{\text{peak}}} \quad (2)$$

where $\Delta \lambda_{\text{peak}}$ is the resonance wavelength difference between the two adjacent analytes resonance peaks and n_a is the refractive index change between the two adjoining analytes.

The equation for the Signal-to-Noise Ratio (SNR), which gages sensor performance, is [20]:

$$\text{SNR} = \frac{\Delta \lambda_{\text{peak}}}{\text{FWHM}} \quad (3)$$

where FWHM is the Full Width at Half Maximum.

The figure of merit (FOM) for optical fibers can be calculated using various formulas, depending on the specific application and the desired characteristics. FOM is expressed as [18]:

$$\text{FOM}\left[\text{RIU}^{-1}\right] = \frac{\text{Sensitivity}\left(\frac{\text{nm}}{\text{RIU}}\right)}{\text{FWHM (nm)}} \quad (4)$$

Experimental procedures

In this experiment, a well-established procedure was followed according to previous work. The optical system for measuring the transferred light spectrum subsists of a laser diode light source (653 nm), SMF, PCF (Thorlabs Co.), Coupler, spectrophotometer (HR4000CG UV-NIR), and drops of Carbonated liquids. The laser diode was connected to a coupler which in turn is connected to the SMF-PCF-SMF. The spectrophotometer is coupled to a computer from one end and to the other end of the SMF-PCF-SMF. Thorlabs' advanced software saves the SPR curves together with the data values and displays them online on the computer screen. A photograph of the established sensor set up is displayed in Fig. 3.

Results and discussion

The presentation of the sensor was evaluated by measuring the refractive indices of combinations of sucrose mixtures at numerous concentrations with an Abbe refractometer. A calibration curve for PCF between the solutions refractive indices and their concentrations is determined in Fig. 4.

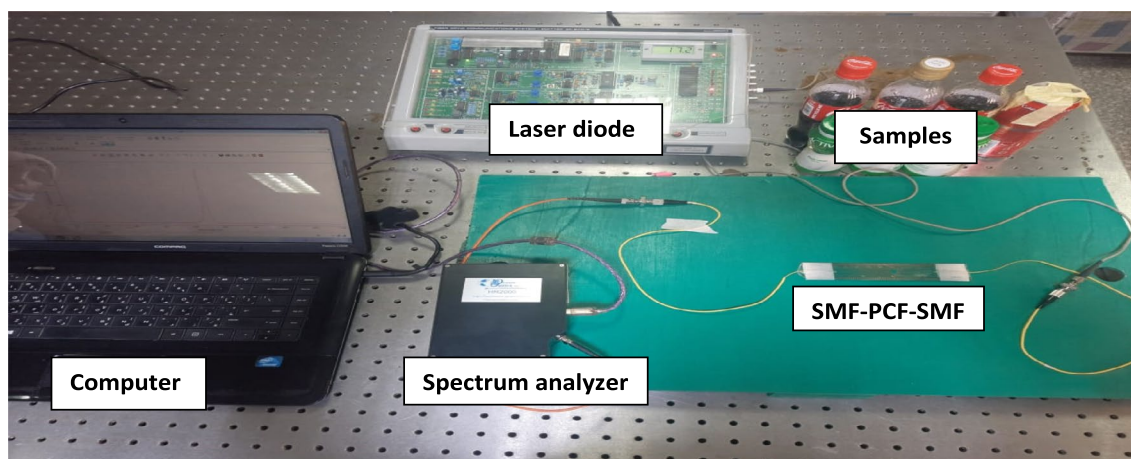When the refractive index of the surrounding medium increases, the resonance wavelength shifts to a longer

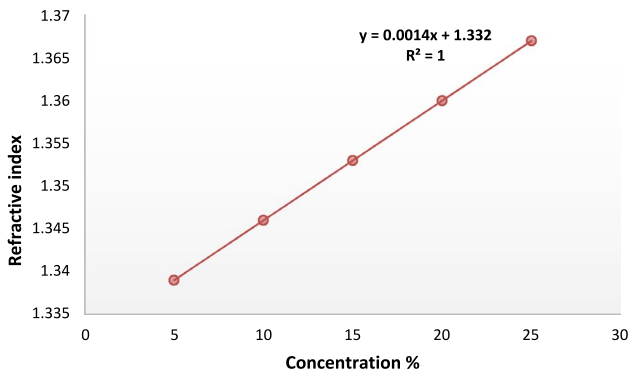**Fig. 3** The experimental setup of SMF-PCF-SMF-based on SPR by using laser diode

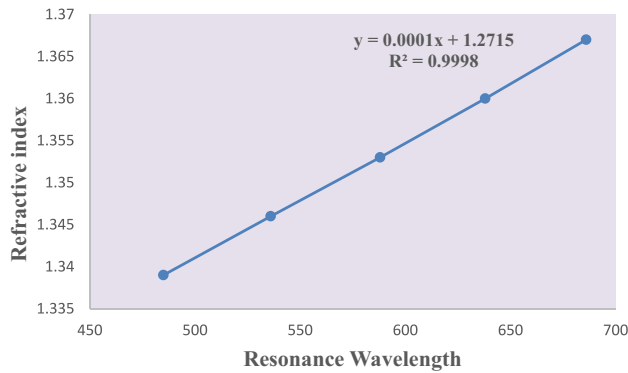**Fig. 4** SMF-PCF-SMF calibration curve using sucrose solutions

Fig. 5 An analysis of the resonance wavelength for gold coated sensors in relation to refractive index

Fig. 6 Shows SPR curve for samples of carbonated liquids with different expiration dates

Table 1 Empirical operation of the instrument

Metal/ (thickness)	Sensitivity [μm/RIU]	Figure of merit (FOM)	Signal-to-noise ratio (SNR)	Resolution [RIU]
Gold/40 nm	7.17	19.14	0.536	1.3×10^{-4}

Table 2 Shows the performance of 4 different samples of carbonated liquids according to the sensor parameters

Sample	(λ_{res}) (nm)	Refractive index (n)	Concentration of the sensor (C) %
A	652	1.3367	3.357
B	653	1.3368	3.428
C	658	1.3373	3.785
D	662	1.3377	4.07

wavelength. This shift is known as a "redshift" as seen in Fig. 5. This sensitivity of the resonance wavelength to changes in the refractive index of the carbonated liquids with different expiration dates forms the basis for SPR-based sensing applications which is displayed in Fig. 6. By monitoring the wavelength shift, it is possible to detect and quantify changes in the refractive index of the surrounding medium. This makes SPR-based sensors valuable tools for label-free and real-time detection of chemical and biological interactions. SPR response curves' dip locations and widths are affected by each sensor's refractive index, and gradient positions become more varied as refractive index declines. Refractive index changes are dependent on the spectral curve's breadth. When the resonance wavelength and refractive index of the sensor are modified, the width, dip location, and shifting value of the surface plasmon resonance curve change. Blank's law, which states that energy is inversely proportional to wavelength, states that an increase in toxic metal ions causes an increase in resonance wavelength, resulting in an increase in refractive index RI [21].

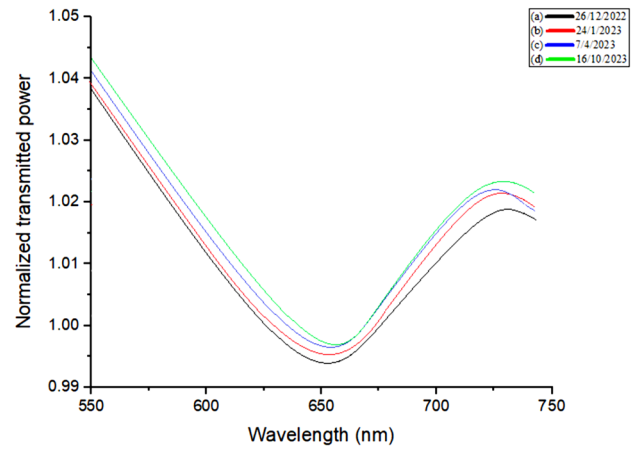As shown in Table 1, the gold sensor has a set of performance parameters corresponding to its performance. Based on the previous equations that were mentioned above, the figure of merit, resolution, sensitivity, and signal-to-noise ratio were calculated. With different expiration dates, carbonated liquids with varying sensor parameters are shown in Table 2.

Conclusion

This work shows the results for sensing of carbonated liquids with different expiration dates when associated with photonic crystal fiber sensor based on surface plasmon resonance. As experimentally tested, the sensor shows the variations of the values of resonant wavelength with refractive indices and concentrations of different carbonated liquid samples. The 40 nm thickness of gold shows effective

performance parameters as the sensitivity reaches 7.17 (μm/RIU), figure of merit is 19.14, signal-to-noise ratio 0.536, and finally resolution at 1.3×10^{-4} (RIU) which means that the Optimization of the gold layer thickness, surface functionalization, and experimental conditions can further enhance the SPR performance parameters for specific applications, such as biosensing, environmental monitoring, and chemical analysis.

References

1. D.C. Zografopoulos, A. Pitilakis, E.E. Kriezis, Liquid crystal-infiltrated photonic crystal fibres for switching applications. Optofluidics Sens. Actuators in Microstruct. Opt. Fibers. **1**, 55–83 (2015)

2. J.M. Dawes, Synthesis, characterization, and applications of opals, Nano-Optics, (2020)

3. J.E. Sharping, P. Kumar, Photonic Crystals | Nonlinear Optics, Photonic Crystal Fibers, Encyclopedia of Modern Optics, (2005)

4. G.M. Jassam, S.S. Ahmed, D-shaped photonic crystal fiber toxic metal ions (arsenic) sensor based on surface Plasmon resonance. Iraq. J. Phys. **21**(2), 91–98 (2023)

5. F. Meng, H. Wang, D. Fang, Research on D-shape open-loop PCF temperature refractive index sensor based on SPR effect. IEEE Photon. J. **14**(3), 1–5 (2022)

6. X. Fan, I.M. White, S.I. Shopova, H. Zhu, J.D. Suter, Y. Sun, Sensitive optical biosensors for unlabeled targets: a review. Anal. Chim. Acta **620**(1–2), 8–26 (2008)

7. J. Lu, T. Van Stappen, D. Spasic, F. Delport, S. Vermeire, A. Gils, J. Lammertyn, Fiber optic-SPR platform for fast and sensitive infliximab detection in serum of inflammatory bowel disease patients. Biosens. Bioelectron. **79**, 173–179 (2016)

8. L. Zhang, M. Fang, Nanomaterials in pollution trace detection and environmental improvement. Nano Today **5**(2), 128–142 (2010)

9. B. Krotkiewska, M. Pasek, H. Krotkiewski, Interaction of glycophorin A with lectins as measured by surface plasmon resonance (SPR). Acta Biochim. Pol. **49**(2), 481–490 (2002)

10. A. Hassani, M. Skorobogatiy, Design of the microstructured optical Fiber-based surface Plasmon resonance sensors with enhanced microfluidics. Opt. Express **14**(24), 11616–11621 (2006)

11. J.N. Dash, R. Jha, Graphene based birefringent photonic crystal fiber sensor using surface plasmon resonance. IEEE Photon. Technol. Lett. **26**(11), 1092–1095 (2014)

12. J. Yao, X. Yang, M. Wang, Y. Lu, Surface plasmon resonance sensor based on hollow-core PCFs filled with silver nanowires. Electron. Lett. **51**(21), 1675–1677 (2015)

13. J. Arriaga, J.C. Knight, and P.ST. Russell, Modeling photonic crystal fibers, Physica E 17, Elsevier Science, pp. 440-442, (2003)

14. S. Soussi, Modeling photonic crystal fibers. Adv. Appl. Math. **36**(3), 288–317 (2006)

15. L. Xiao, M.S. Demokan, W. Jin, Y. Wang, C.L. Zhao, Fusion splicing photonic crystal fibers and conventional single-mode fibers: microhole collapse effect. J. Lightwave Technol. **25**(11), 3563–3574 (2007)

16. A.I. Mahmood, A.I. Mahmood, S.S. Ahmed, Refractive index sensor based on micro structured optical fibers with using finite element method. Iraq. J. Sci. **59**(3C), 1577–1586 (2018)

17. S. Silva, P. Roriz, and O. Frazão. Refractive index measurement of liquids based on microstructured optical fibers. Photonics, (2014)

18. F.F. Abbas, S.S. Ahmed, Photonic crystal Fiber pollution sensor based on surface Plasmon resonance. Iraq. J. Sci. **64**(2), 658–667 (2023)

19. F.F. Abbas, S.S. Ahmed, Photonic crystal fiber pollution sensor based on the surface Plasmon resonance technology. Baghdad Sci. J. **20**(2), 0452 (2023)

20. N.S. Rahim, S.S. Ahmed, M.F. Sultan, Optical fiber biomedical sensor based on surface Plasmon resonance. Iraq. J. Sci. **61**(7), 1650–1656 (2020)

21. G.M. Jassam, S.S Ahmed, Estimating concentration of toxic ions arsenic in water by using photonic crystal fiber based on surface Plasmon resonance (SPR). Baghdad J. Sci. (2023)